# Phase separation and crystallization of La2O3 doped ZnO-B2O3-SiO2 glass

WANG, M., FANG, L., LI, M., LIU, Z., HU, Y., ZHANG, X., DENG, Wei and DONGOL, R.



**Published version**

WANG, M., FANG, L., LI, M., LIU, Z., HU, Y., ZHANG, X., DENG, Wei and DONGOL, R. (2019). Phase separation and crystallization of La2O3 doped ZnO-B2O3-SiO2 glass. Journal of Rare Earths.

**Copyright and re-use policy**

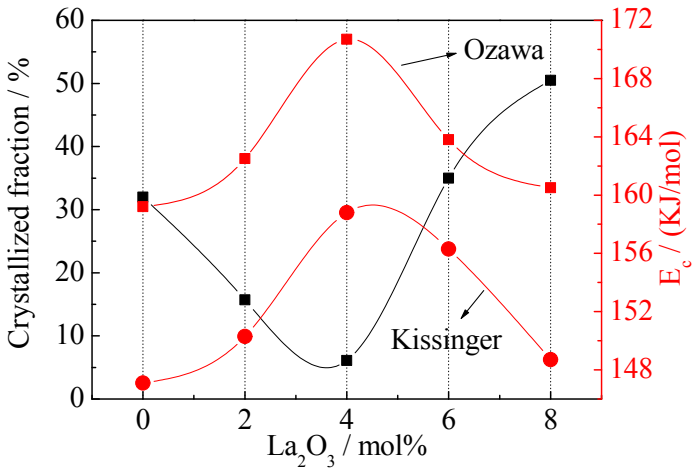


The dependence of the crystallization activation energy $E_c$ of 60ZnO-30$B_2O_3$-10$SiO_2$ glass on the $La_2O_3$ doping amount is illustrated in Figure, the change trend of $E_c$ values estimated by Ozawa and Kissinger methods is same, as the doping amount of $La_2O_3$ increases from 0 to 8 mol%, the maximum value of crystallization activation energy $E_c$ appears at 4 mol% of $La_2O_3$, indicating that the crystallization barrier need to overcome is largest for glass doped with 4 mol% of $La_2O_3$ , as a result, the crystallization of glass is inhibited. This result can be used to control the depth of crystal layer at glass surface, crystallinity and thermal stability of 60ZnO-30$B_2O_3$-10$SiO_2$ glass by doping with different content of $La_2O_3$.

# Phase separation and crystallization of $La_2O_3$doped $ZnO-B_2O_3-SiO_2$ glass

Mitang Wang[1, 2]*, Long Fang[1, 2], Mei Li[1, 2], Zhaogang Liu[1, 2], Yanhong Hu[1, 2], Xiaowei Zhang[1, 2], Wei Deng[3], Ruhil Dongol[4]

([1]School of Materials and Metallurgy, Inner Mongolia University of Science & Technology, Baotou 014010, China;
[2]Key Laboratory of Green Extraction & Efficient Utilization of Light Rare-Earth Resources, Ministry of Education, Baotou 014010, China;
[3]Materials EngineeringMaterials and Engineering Research Institute, Sheffield Hallam University, SheffieldS1 1WB, UK;
[4]New York State College of Ceramics, Alfred University, Alfred, NY, 14802, USA)

Corresponding author: M.T. Wang
Email: btwmt@126.com
Tel: 086-15848255894

**Abstract:** In order to investigate the effect of the $La_2O_3$ on the phase separation and crystallization of $ZnO-B_2O_3-SiO_2$ glass, after the occurence of the phase separation and crystallization of glasses by heat treatment, the microstructure morphology and distribution of elements in different sample areas were characterized by the scanning electron microscopy (SEM) and energy dispersive spectroscopy (EDS); the non-isothermal crystallization kinetics of the glass samples was studied by using a differential scanning calorimeter (DSC) and the precipitated crystals of crystallized glass were determined by the X-ray diffraction (XRD). The results suggest that the phase separation and crystallization of $60ZnO-30B_2O_3-10SiO_2$ glass occur at glass surface, and the incorporation of small amount (< 4 mol%) of $La_2O_3$ significantly inhibits the glass phase separation and consequently improves the thermal stability of glass. Doping of $La_2O_3$accelerates the glass crystallization at the elevated temperature (660 ºC), making the depth of crystal layer thicker and diffraction intensity in XRD patterns stronger. However, due to the precipitation of several crystals that occur simultaneously when $La_2O_3$ doping amount is 4mol%, crystallization of the $60ZnO-30B_2O_3-10SiO_2$ glass is obviously depressed, the crystallization activation energy $E_c$ and the relative crystallinity $X_c$ of the glass reach the maximum and the minimum values, respectively. Although transition from one-dimensional growth of crystals to two-dimensional growth of crystals results from $La_2O_3$ addition, the one-dimensional growth of crystals remains dominant in crystallization process. This work can provide some useful information for preparing glass ceramics with nano-crystals precipitated in the glass surface.

**Keywords:** zinc borosilicate glass;$La_2O_3$;phase separation; crystallization; rare earths

## 1. Introduction

ZnO based materials have been extensively applied in the field of optoelectronic devices, gas sensor, catalyst and new energy materials due to the semiconducting properties of zinc oxides [1, 2]. Meanwhile, glasses in the composition of $ZnO-B_2O_3-SiO_2$ system have attracted numerous attention in luminescent, optical storage, solid laser and sealing areas because of the excellent optical properties, low thermal expansion coefficient and melting temperature [3, 4]. The properties of glass mainly depend on the structure given by its specific chemical compositions. It is well known that $SiO_2$ and $B_2O_3$ are the typical glass network former, silicon atom present in form of [$SiO_4$], boron existing in [$BO_3$] and [$BO_4$], depend on the specific chemical composition of glass. The coordination numbers of zinc in glass could be 4 and 6,

which is named as network intermediate. Zinc oxide has dual role in the glass structure, increases the connectivity of glass structure as zinc exists in [$ZnO_4$], and provides non-bridging oxygen and makes the glass structure open when coordination number of zinc is 6 [5]. As for optical materials, rare earth elements with abundant of energy levels are commonly incorporated into glass to tailor the luminescent properties of optical materials [6-11]. Rare earth ions always exist in glass as network modifier, and it has higher cationic field strength, which has strong effect on the basic building units in glass structure and makes the order and disorder state of local structure more complicated, consequently results in the occurence of phase separation and crystallization of glass containing rare earth elements [12]. It was reported that, addition of rare earth oxides such as $La_2O_3$, $CeO_2$, $Nd_2O_3$, $Eu_2O_3$ and $Y_2O_3$ has significant impact on the nucleation and crystal growth of MgO-$Al_2O_3$-$SiO_2$, $Li_2O$-$Al_2O_3$-$SiO_2$, $La_2O_3$-$B_2O_3$ and $Li_2O$-$SiO_2$ glasses [13-15]. Apart from the effect of rare earth elements on the microstructure of glass structure, competition of B and Zn for oxygen to satisfy their coordination requirements and different structure between[$BO_3$] and [$SiO_4$] units make the phase separation and crystallization of ZnO-$B_2O_3$-$SiO_2$ system glass much more easy to occur during process[5, 16], as a result, thermal stability and glass forming ability of ZnO-$B_2O_3$-$SiO_2$ system glass, specially for the glass containing high amount of ZnO and $B_2O_3$, are deteriorated seriously[16]. Thereby, it is interesting to explore the effect of rare earth elements on the phase separation and crystallization of ZnO-$B_2O_3$-$SiO_2$ system glass. In our previous work [16], it shows that different contents of $La_2O_3$ and $Y_2O_3$ doping into ZnO-$B_2O_3$-$SiO_2$ system glass has different influence on the glass forming ability due to their effect on the conversion of [$BO_3$] and [$BO_4$], [$ZnO_4$] and [$ZnO_6$]. Thereby, the objective of this work is to investigate the effect of the $La_2O_3$ on the phase separation and crystallization of ZnO-$B_2O_3$-$SiO_2$ glass, the microstructure morphology and the distribution of elements in the different areas after phase separation, and crystallization of glasses heat treatedare characterized by SEMequipped with EDS, as well crystallization kinetics of the glass were studied by non-isothermal methods.

## 2 Experimental

### 2.1 Glass preparation

60ZnO-30$B_2O_3$-10$SiO_2$ glasses doped with different contents of $La_2O_3$ (2 mol%, 4 mol%, 6 mol% and 8 mol%) were prepared by melt quenching method. The used raw materials were analytical grade reagents including boric acid, ZnO, $SiO_2$ and $La_2O_3$. To be simple, the prepared glass samples were named as B0 for glass doped without $La_2O_3$, L1, L2, L3 and L4 for glass doped with $La_2O_3$. After mixing thoroughly, 100 g of batch in the platinum crucible was melted in electric furnace at 1100–1300 ºC for 1–2 h depending on the glass chemical composition, followed by annealing at 550 ºC in a furnace for 1h, and then naturally cooled down to room temperature. Annealed glasses were cut into regular samples of 5 mm×10 mm×20 mm, and heat treated by specific thermal schedule for the study requirements of phase separation and crystallization of glass, and the specific heat treatment schedules were determined on the basis of sample thermal analysis. By cutting and polishing of heat treated glasses the samples for observing phase separation and crystallization behaviors were obtained.

### 2.2 Characterization

To obtain the glass transition temperature $T_g$ and crystallization temperature $T_p$ of glass, the thermal analysis for grinded glass powder was carried out by a differential scanning calorimeter (DSC, Model STA449C, Germany). The glass powders were heated in nitrogen atmosphere from room temperature to 900 ºC with

different heating rates ($\beta$=5, 10, 15 and 20 ºC/min). The measurement error of $T_g$ and $T_p$ values is ±1 ºC. To observe the morphology of phase separation occurred and the crystallite phase precipitated in the glass, the measured surfaces of the samples were polished and then eroded in the 4.0 wt% HF acid solution for 10-30s. After cleaning with deionized water and dry in air, the measured surfaces sprayed with a layer of gold were performed by scanning electron microscopy analysis (SEM FEI QUANTA-400 and ZEISS Sigma 500). Meanwhile, the distribution of elements in the different areas after phase separation and crystallization of glasses heat treated were characterized by EDS. The precipitated crystallites of the heat treated specimens were identified by the an X-ray powder diffractometer (XRD, Model QUEST, America), using Cu Kα radiation. The XRD patterns were recorded in 2$\theta$ range of 10°–80° at the step size of 0.04. The XRD data were analyzed using Jade software.

## 3 Results and discussion

### 3.1 DSC analysis

Fig. 1 illustrates the DSC curves for glass samples B0, L1, L2, L3 and L4 at heating rate of 5, 10, 15 and 20 ºC/min. It is observed that glass transition temperature $T_g$ and crystallization temperature $T_p$ for all glasses shift to higher temperature with increase of heating rate, which is in agreement with the results reported by other researchers [17–19]. For base glass B0, there are two distinct exothermic peaks $T_{p1}$ and $T_{p2}$, as shown in Fig. 1(a), $T_{p1}$ is of 725 ºC and $T_{p2}$ 760 ºC for the DSC curve carried out at heating rate of 10 ºC/min. Two exothermic peaks present in DCS measurements suggest that there are transformation of crystal form or simultaneous precipitation of different crystal in zinc borosilicate base glass when heat treatment is carried out on it. While there is one exothermic peak for $La_2O_3$ doped glass as shown in Fig. 1(b–e).

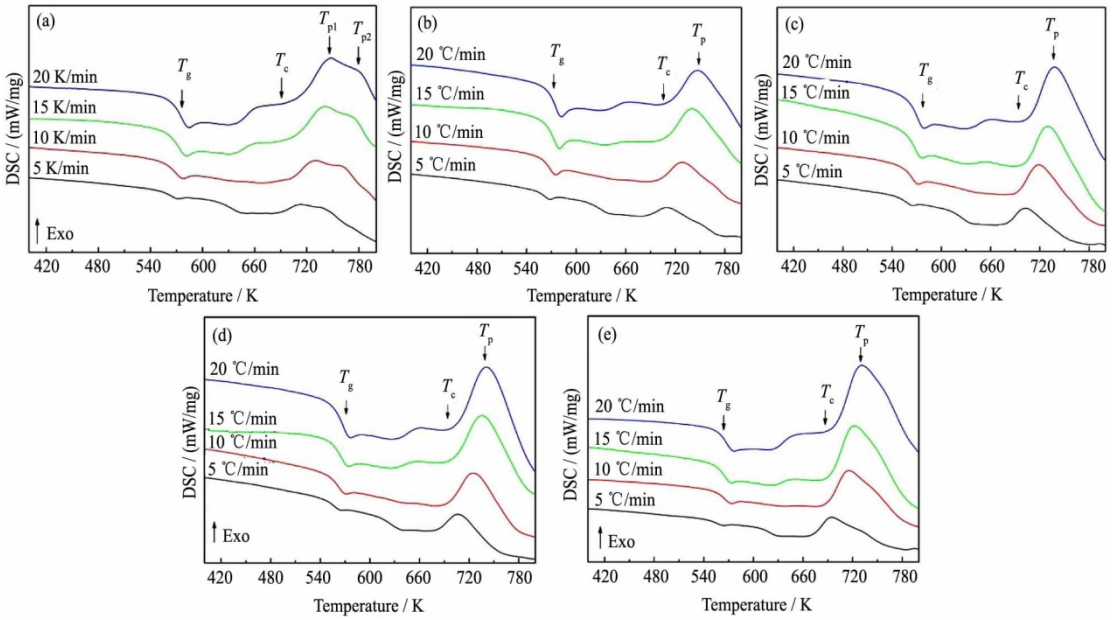


Fig.1 DSC curves of the glasses samples. (a) B0; (b) L1; (c) L2; (d) L3; (e) L4.

### 3.2Phase separation of parent glass

It is well known that the occurence of glass phase separation can be observed by heat treating the glass at the temperature close to glass transition temperature $T_g$[20]. Glass transition temperature of 60ZnO-30$B_2O_3$-10$SiO_2$ parent glass is about 570 ºC when the heating rate is 10 ºC/min, as shown in Fig. 1(a). Thereby, the parent glass B0 were heat treated at temperatures of 620 and 640 ºC, respectively for 5 or 10 h,

and the phase separation of glass B0 are given in Fig. 2. It is found that the phase separation of glass B0 occurs at the glass surface, and the morphology of phase separation is mainly wormlike along with a few of isolated droplets. Comparing the glass B0 heat treated at 620℃ for 5h (Fig.2 (a)) with glass B0 at 640 ºC for 5 h (Fig. 2(b)), the phase separation becomes more severe with the increase of heat treatment temperature from 620 to 640 ºC when keep the duration of heat treatment constant, which is mainly due to the easier structure rearrangement caused by the open glass structure as the temperature increases. When keeping the teat treatment temperature at 640 ºC, the phase separation of glass B0 gets more serious with prolonging the teat treatment time from 5 to 10 h, as shown in Fig. 2(b) and (c). Besides, a few crystals are precipitated as illustrated in framed area in Fig. 2(c), in order to obtain the detail information about crystallization behavior, the magnified view of the framed region in Fig. 2(c) is given in Fig. 2(d). It suggests that the crystal growth along with the interfaces between the two phases caused by heat treatment, orients to the inside of glass and extends to the in walls of phases. The way of crystal nucleation and growth mainly correlates with two factors. On the one hand, the larger surface area of interface caused by phase separation makes the nucleation occur easier at the interface, on the other hand the components in one phase is really similar with the components of crystal precipitated in the interface between two phases, as a result decreasing the nucleation activation energy and facilitating the nucleation and crystal growth [21].Due to the larger surface area and more structure defect near glass surface, and there is not nucleating agent in glass chemical compositions, the phase separation easier occurred near glass surface rather than glass bulk, and phase separation facilitates the crystallization.

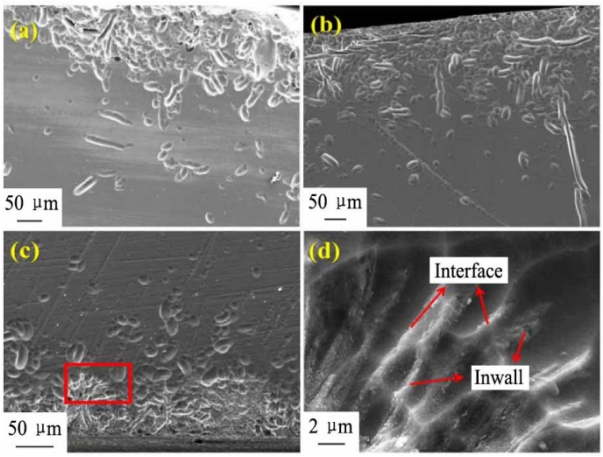


Fig. 2 The SEM images of phase separated B0 glass. (a) Glass B0 heat treated at 620 ºC for 5 h; (b) Glass B0 at 640 ºC for 5 h; (c) Glass B0 at 640 ºC for 10 h; (d) The enlarged view of the red region in fig(c).

3.3 Phase separation and crystallization of $La_2O_3$containing glass

$60ZnO\text{-}30B_2O_3\text{-}10SiO_2$ glasses doped with different contents of $La_2O_3$ were heat treated at 620 ºC for 5 h to observe the variation of phase separation of glass. As shown in Fig. 3, comparing with Fig. 2, phase separation of glass is significantly inhibited as doping content of $La_2O_3$ is less than 4 mol% (Fig.3 (a) and (b)), while more than 4 mol%, the phase separation becomes serious, and is accompanied with precipitation of crystals (Fig. 3(c) and (d)). It is obvious that the extent of crystallization increases with increase of $La_2O_3$ doping content in parent glass when

comparing Fig. 3(c) with (d). Additionally, the phase separation and crystallization keep occurring at the glass surface, indicating that the addition of $La_2O_3$ into glass has slight influence on the mechanism of phase separation and crystallization of 60ZnO-30$B_2O_3$-10$SiO_2$parent glass, and it can be concluded that phase separation of 60ZnO-30$B_2O_3$-10$SiO_2$glass can be depressed when a small amount of $La_2O_3$ (< 4 mol%) is added into glass, in turn improves the thermal stability of glass which has been reported in our previous study [16], while the doping content of $La_2O_3$ is more than 4 mol%, the crystallization of 60ZnO-30$B_2O_3$-10$SiO_2$glass can be accelerated maybe because $La_2O_3$ acts as nucleating agent in glass, thereby the thermal stability of glass deteriorates [13,14].

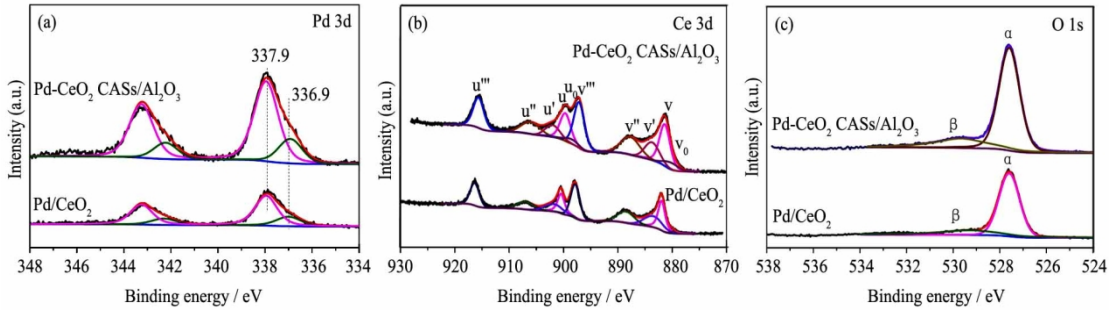


Fig. 3 SEM micrographs showing the surface microstructure of the glass doped with $La_2O_3$ heat treated at 620 ºC for 5 h.

To determine the distribution of glass components such as La and other elements after phase separation and crystallization, backscattered scanning and energy dispersive spectroscopy for glass L4 subjected heat treatment at 640 ºC for 5 h, polishing and gold sputtering, was carried out and the results are illustrated in Fig. 4. It can be seen from Fig. 4(a) that slight phase separation and obvious dendritic crystal are formed at the glass surface, suggesting that distribution of glass components in the dark and slight grey regions is different. Fig. 4(c) and (d) give the EDS results for A (dark grey region) and B (slight grey region) areas in Fig. 4(b), and the specific distribution of glass components are listed in Table 1. Comparing the elements contents in A and B regions, B region is mainly rich in La and Si, while A region is mainly rich in Zn, and according to XRD results (next section) the B also aggregates in dark grey region, which suggests that regions rich in La and Si as well as Zn and B are formed in 60ZnO-30$B_2O_3$-10$SiO_2$glass by phase separation and crystallization.

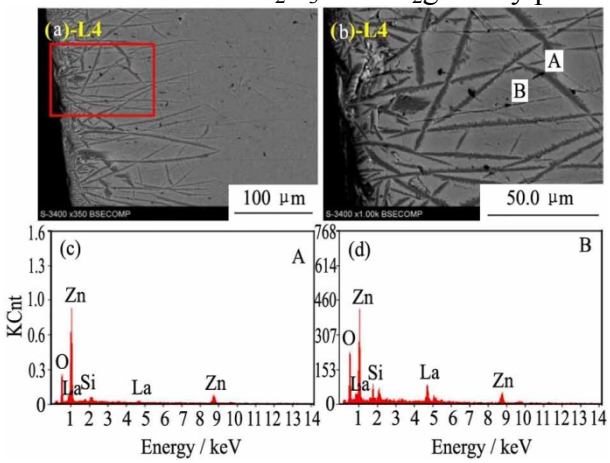


Fig.4 The backscattered electron scanning images of samples L4 heat treated at 640℃ for 5 h. (a) The microscopic appearance of glass samples; (b) The amplification of Fig. (a); (c and d) EDS patterns of marked areas A and B

Table 1 Distribution of element content of different region caused by phase separation

| Element | Mass fraction | | Atom fraction | |
|---|---|---|---|---|
| | A | B | A | B |
| O | 17.14 | 13.43 | 46.28 | 42.85 |
| Si | 2.29 | 5.16 | 3.52 | 9.37 |
| La | 8.9 | 38.17 | 2.71 | 14.02 |
| Zn | 71.86 | 43.23 | 47.49 | 33.75 |

It has been demonstrated that the crystallization occurs for the $60ZnO\text{-}30B_2O_3\text{-}10SiO_2$ glass doped with more than 4 mol% $La_2O_3$ when heat treatment was done at 620 ºC for 5 h. To further investigate the effect of $La_2O_3$ content on the crystallization of $60ZnO\text{-}30B_2O_3\text{-}10SiO_2$glass, glasses doped with different contents of $La_2O_3$ were heat treated at elevated temperature (660 ºC for 5 h), the variation of crystallization behavior performed at the glass surface. Fig. 5 shows the surface microstructure of the glass samples heat treated at 660 ºC for 5 h. Crystallization for all glasses occurs at their surface and precipitated crystals are dendritic and orient inside of glass, incorporation of $La_2O_3$ accelerates the crystallization of glass and makes the precipitated crystals more fine and close when comparing with the glass B0. Additionally, the depth of crystal layer precipitated at the glass surface increases from about 172.4 μm for B0 to 1111 μm for L4 as the doping amount of $La_2O_3$ increases from 0 to 8 mol%, indicating that except glass L2 as shown in Fig. 5(c), crystal layer depth increases with increase of $La_2O_3$ content. Fig. 6 presents the XRD patterns of all glasses heat treated at 660 ºC for 5 h. It shows that the diffraction intensity in XRD patterns increases with the increase in $La_2O_3$ amount, however, the diffraction intensity in XRD patterns for sample L2 is not increased obviously, which is in agreement with the results depth of crystal layer at glass surface. From the XRD patterns, one can also find that the main crystallite phase is $Zn_3B_2O_6$ for glass B0, as doping content of $La_2O_3$ in parent glass increases up to 4 mol%, the crystallites $LaBO_3$ and $Zn_2SiO_4$ begin to precipitate simultaneously with $Zn_3B_2O_6$, this might be the reason for slight decrease of crystal layer depth and diffraction intensity for glass L2 comparing with other glass doped with $La_2O_3$, potential barrier for crystallization for glass L2 becomes larger due to several crystals precipitated simultaneously, nucleation and crystal growth consequently are inhibited [13,14, 22].

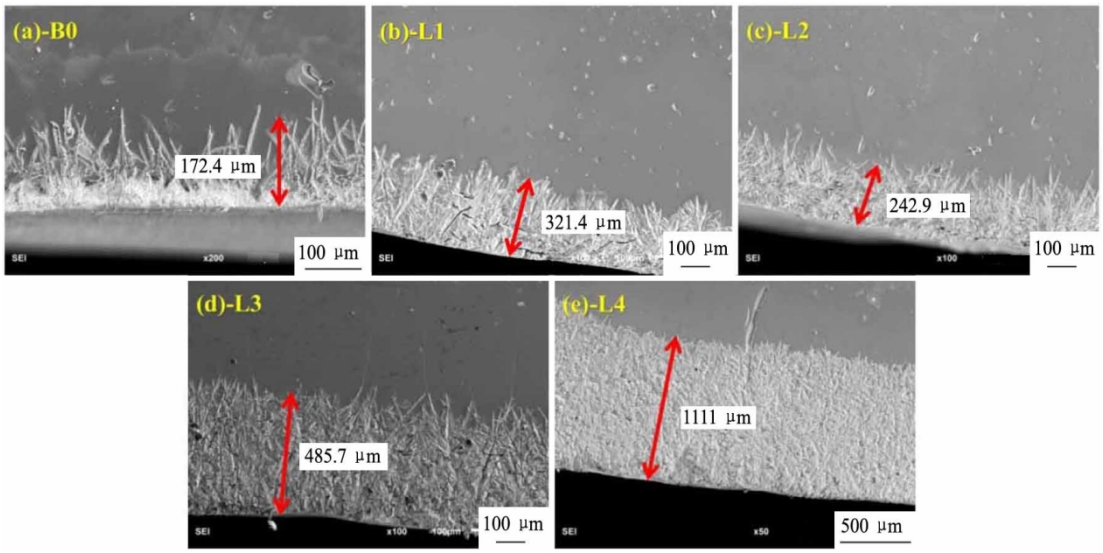


Fig.5 SEM micrographs showing the surface microstructure of the glass samples heat treated at 660 ℃ for 5 h.

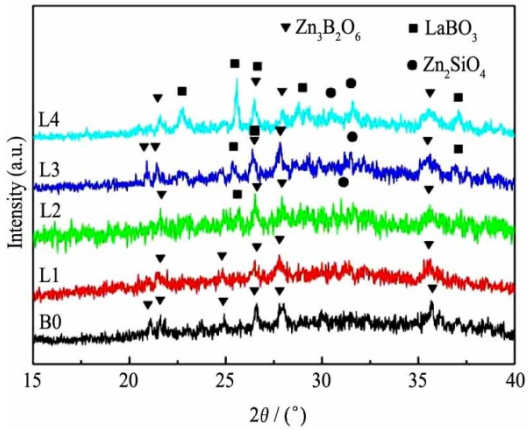


Fig.6 XRD patterns of different amount of $La_2O_3$ doped glass samples

To quantitatively characterize the effect of $La_2O_3$ on the crystallization degree of $60ZnO\text{-}30B_2O_3\text{-}10SiO_2$ glass, crystallinity $X_c$ defined as the ratio of precipitated crystals volume to original volume of glass is calculated by following expression on the basis of XRD data [23,24].

$$X_c = \frac{I_c}{I_c + I_a} \times 100\% \quad (1)$$

where $I_a$ is integral sum of all diffuse peak, $I_c$ is integral sum of all crystal peak in XRD patterns. $I_a$, $I_c$ and $X_c$ are values calculated on the basis of XRD results as shown in Fig. 6 are listed in Table 2. The dependence of glass crystallinity on the $La_2O_3$ doping amount is given in Fig. 7, the crystallinity of glass decreases firstly and then increases with increasing of $La_2O_3$ content from 0 to 8 mol%, minimum value for glass crystallinity appears at glass L2 doped with 4 mol% $La_2O_3$. This is mainly due to the variation of potential barrier for glass nucleation and crystal growth caused by the incorporation $La_2O_3$ in $60ZnO\text{-}30B_2O_3\text{-}10SiO_2$ glass, which will be discussed in next section.

Table 2 The $I_a$, $I_c$ and $X_c$ values of glasses calculated from the XRD pattern

| Glass | $T$/℃ | $t$/h | $I_a$ (a.u.) | $I_c$ (a.u.) | $X_c$/% |
|---|---|---|---|---|---|
| B0 | 660 | 5 | 11687 | 5528 | 32.0 |
| L1 | 660 | 5 | 10157 | 1888 | 15.7 |
| L2 | 660 | 5 | 15827 | 1030 | 6.1 |
| L3 | 660 | 5 | 5149 | 2771 | 35.0 |
| L4 | 660 | 5 | 3705 | 3775 | 50.5 |

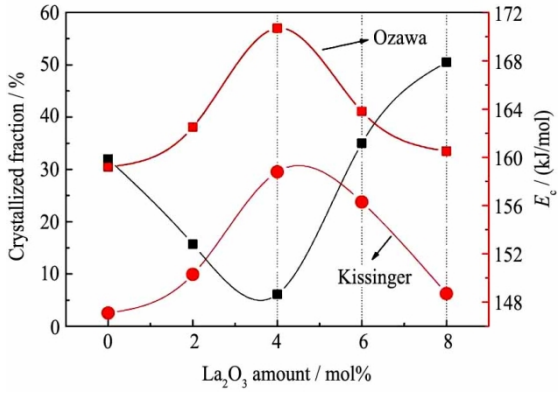


Fig.7 The crystallinity and crystallization activation energy of $La_2O_3$ doped glass samples

3.4 Crystallization kinetics

The difficulty of glass crystallization can be characterized by the crystallization activation energy, glass structure rearrangement when glass transforms into crystals needs to overcome the crystallization barrier which is defined as crystallization activation energy $E_c$. The larger the crystallization activation energy, the higher the crystallization barrier needs to overcome; nucleation and crystal growth rates become slowly, consequently the crystallization of glass is depressed [25,26]. To quantitatively explore the effect of $La_2O_3$ doping amount on the crystallization activation energy $E_c$ of $60ZnO\text{-}30B_2O_3\text{-}10SiO_2$ glass, two expressions were used to estimate the $E_c$ value. One is the Kissinger equation [26,27],

$$\ln(\beta / T_p^2) = \text{cons tan } t - E_c / RT_p \quad (2)$$

The other is Ozawa expression [28] as following,

$$\ln\beta = \text{cons tan } t - E_c / RT_p \quad (3)$$

Where $\beta$ is heating rate, $T_p$ crystallization peak temperature, $R$ gas constant. And according to the specific experimental data, the ln ($\beta/T_p^2$) versus $1000/T_p$ and ln $\beta$ versus $1000/T_p$ plots (as shown in Fig. 8) for parent and $La_2O_3$ doped sample at different heating rates are fitted on the basis of Kissinger (Fig. 8(a)) and Ozawa (Fig. 8 (b)) equations, the crystallization activation energy can be obtained from the slope $E_c/R$ of lines and summarized in Table 3. For comparison, the dependence of the crystallization activation energy $E_c$ of $60ZnO\text{-}30B_2O_3\text{-}10SiO_2$ glass on the $La_2O_3$ doping amount is illustrated in Fig. 7, the value of $E_c$ obtained by Ozawa method is larger than that by Kissinger, but the change trend of $E_c$ values estimated by two different methods is the same, $E_c$ values increase firstly from 147.1 to 158.8 kJ/mol and then decreases to 148.7 kJ/mol for Kissinger method, 159.2 to 170.7 then to 160.5 kJ/mol for Ozawa method as the doping amount of $La_2O_3$ increases from 0 to 8 mol%, the maximum value of crystallization activation energy $E_c$ appears at 4 mol% $La_2O_3$,

indicating that the crystallization barrier that needs to overcome is the largest for glass L2, as a result, the crystal nucleation and crystallization in glass L2 is inhibited because the several crystals ($Zn_3B_2O_6$, $LaBO_3$ and $Zn_2SiO_4$)are precipitated simultaneously as shown in Fig. 6. This can be used to explain variation trends for the depth of crystal layer at glass surface, X-ray diffraction intensity and crystallinity of 60ZnO-30$B_2O_3$-10$SiO_2$ glass doped with different contents of $La_2O_3$. This also suggests that crystallization of glass L2 is the hardest comparing with other $La_2O_3$ doped glasses, namely its thermal stability is the best, which is in good agreement with our previous results characterized by parameter $S$ [16]. It can be concluded that the crystallization and thermal stability of 60ZnO-30$B_2O_3$-10$SiO_2$ glass can be depressed and improved by doping less than 4 mol% $La_2O_3$, while introduction of more than 4 mol% $La_2O_3$ facilitates the crystallization behavior of this glass.

Table 3 The crystallization activation energy $E_c$ and crystal growth parameter $n$.

| Glass | $E_c$（kJ/mol） | | $n$ | $m$ |
|---|---|---|---|---|
| | Kissinger | Ozawa | Kissinger | |
| B0 | 147.1 | 159.2 | 2.00 | 1 |
| L1 | 150.3 | 162.5 | 2.12 | 1 |
| L2 | 158.8 | 170.7 | 2.10 | 1 |
| L3 | 152.1 | 163.8 | 2.08 | 1 |
| L4 | 148.7 | 160.5 | 2.48 | 1 |

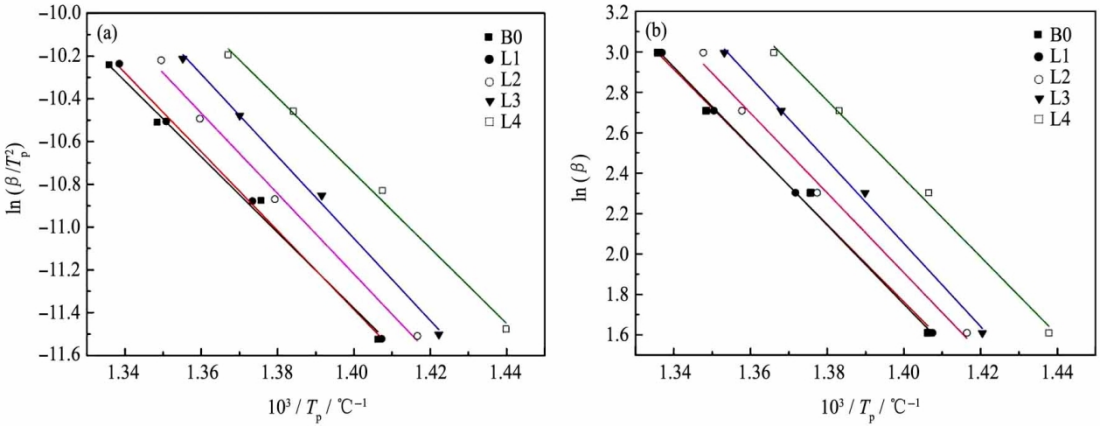


Fig. 8 (a) ln($\beta/T_p^2$) versus 1000/$T_p$ plots for B0, L1, L2, L3 and L4 samples at different heating rates; (b) ln $\beta$ versus 1000/$T_p$ plots.

The mechanism for the crystallization of 60ZnO-30$B_2O_3$-10$SiO_2$glass doped with different contents of $La_2O_3$ is calculated by Augis–Bennett equation[29],

$$n = \frac{2.5}{\Delta T} \cdot \frac{RT_p^2}{E_c} \quad (4)$$

where n is Avrami index correlated with phase transformation mechanism; $\Delta T$ is the full width at half maximum of the exothermical peak in DSC curve. The $n$ values obtained from Kissinger results and specific experimental data are shown in Fig. 1, and $m$ calculated according to n value [30] is as well listed in Table 3. Values of $n$ and $m$ for parent glass are 2 and 1, indicating that both one-dimensional growth of crystals and surface crystallization mechanisms occur in glassy to crystalline transformation of 60ZnO-30$B_2O_3$-10$SiO_2$parent glass. With incorporation of $La_2O_3$ into parent glass,

the Avramiexponents *n* is more than 2, and *m* approximate to 1, suggesting that transition from one-dimensional growth of crystals to two-dimensional growth of crystals occurs at glass surface, but the one-dimensional growth of crystals remains dominant in crystallization process. These are consistent with the crystallization behavior as shown in Fig. 5.

## 4 Conclusions

The influence of $La_2O_3$ on the phase separation and crystallization behavior of $60ZnO\text{-}30B_2O_3\text{-}10SiO_2$ glass was investigated in this work, the phase separation and crystallization of $60ZnO\text{-}30B_2O_3\text{-}10SiO_2$ glass occur at glass surface when glasses are heat treated at about glass transition temperature, and the incorporation of small amount (< 4 mol%) of $La_2O_3$ significantly inhibits the glass phase separation and thus improves the thermal stability of glass. The depth of crystal layer and diffraction intensity in XRD patterns of all glasses heat treated at 660 ºC for 5 h, show that doping of$La_2O_3$ accelerates the crystallization of parent glass, however, the diffraction intensity in XRD patterns for sample L2 (4 mol% $La_2O_3$) is not increased obviously due to crystallites $LaBO_3$ and $Zn_2SiO_4$ begin to precipitate simultaneously with $Zn_3B_2O_6$. Crystallization kinetics results indicate that as the doping amount of $La_2O_3$ increases from 0 to 8 mol%, the crystallization activation energy increases firstly and then decreases, the maximum value of crystallization activation energy appears at 4 mol% $La_2O_3$, indicating that the crystallization barrier needing to overcome is the largest for glass L2. And transition from one-dimensional growth of crystals to two-dimensional growth of crystals occurs at glass surface, but the one-dimensional growth of crystals remains dominant in crystallization process.

Foundation item: Project supported by National Natural Science Foundation of China (51662033, 51362019) and Natural Science Foundation of the Inner Mongolia Autonomous Region (2016JQ05).

References:

[1] Masai H, Toda T, Ueno T, Takahashi Y, Fujiwara T. ZnO glass ceramics: An alternative way to produce semiconductor materials. Appl Phys Lett. 2009; 94(15): 151908.

[2] Uma V, Marimuthu K, Muralidharan G. Effect of ZnO on the spectroscopic properties of $Dy^{3+}$ doped zinc telluroborate glasses for white light generation. J Non-Cryst Solids. 2018; 498: 386.

[3] Shen Y, Hou L Y, Zuo G F, Li FF, Meng YZ. Preparation of $ZnO–B_2O_3–SiO_2$: $Mn^{2+}$ optical–storage glass–ceramics with different $ZnF_2$ dopant by sol–gel method. J Sol-Gel Sci Technol, 2015, 73(1): 192.

[4] Annapurna K, Dwivedi R N, Kundu P, Buddhudu, S. Blue emission spectrum of $Ce^{3+}$: $ZnO–B_2O_3–SiO_2$ optical glass. Mater Lett. 2004; 58(5): 787.

[5] Cetinkaya C S, Akyuz I, Atay F. On the dual role of ZnO in zinc borate glasses. J Non-Cryst Solids, 2016; 432: 406.

[6] Zeng P, Cao ZM, Chen YH, Yin M. Investigation of the temperature characteristic in $SrB_4O_7$:$Sm^{2+}$ phosphor-in-glass by analyzing the lifetime of 684 nm. J Rare Earths, 2017; 35(8): 783.

[7]Wantana N, Kaewjaeng S, Kothan S, Kim HJ, Kaewkhao J. Energy transfer from $Gd^{3+}$ to $Sm^{3+}$ and luminescence characteristics of $CaO–Gd_2O_3–SiO_2–B_2O_3$ scintillating glasses. J Lumine, 2017; 181: 382.

[8]Man XQ, Yu LX, Sun JJ, Li SC, Zhong JL. Synthesis and photoluminescent properties of $Eu^{3+}/Dy^{3+}$ doped $SrO\text{-}Al_2O_3\text{-}SiO_2$ glass-ceramics. J Rare Earths, 2017; 35(5): 446.
[9] Hu FF, Zhao ZM, Chi FF, Wei XT, Yin M. Structural characterization and temperature-dependent luminescence of $CaF_2:Tb^{3+}/Eu^{3+}$ glass ceramics. J Rare Earths, 2017; 35(6): 536.
[10] Kemere M, SpergaJ, Rogulis U. Luminescence properties of Eu, $RE^{3+}$ (RE =Dy, Sm, Tb) co-doped oxyfluoride glasses and glass–ceramics. J Lumin, 2017; 181: 25.
[11] Ramachari D, Moorthy L R, JayasankarC K. Energy transfer and photoluminescence properties of $Dy^{3+}/Tb^{3+}$co-doped oxyfluorosilicate glass–ceramics for solid-state white lighting. Ceram Int. 2014; 40(7): 11115.
[12]Elodie N, Sophie S, Frederic A, Charpentier T, Jollivet P, Le Gac A, et al. Phase separation and crystallization effects on the structure and durability of molybdenum borosilicate glass. J Non-Cryst Solids. 2015;472(3):120.
[13] Pytalev DS, Caurant D, Majerus O, Tregouet H, Charpentier T, Mavrin, BN. Structure and crystallization behavior of $La_2O_3{\cdot}3B_2O_3$metaborate glasses doped with $Nd^{3+}$ or $Eu^{3+}$ ions. J Alloys Compd. 2015; 641: 43.
[14] Lu P, Zheng Y, Cheng JS, Guo DY. Effect of $La_2O_3$ addition on crystallization and properties of $Li_2O–Al_2O_3–SiO_2$ glass–ceramics. Ceram Int. 2013; 39(7): 8207.
[15] Katrin T, Christian R. $CeO_2$ and $Y_2O_3$ as nucleation inhibitors in lithium disilicateglasses. J Mater Sci. 2016; 51(2):989.
[16] Wang MT, Fang L, Li M, Liu ZG, Hu YH, Zhang XW. Effect of rare earth on thermal stability and glass structure of $ZnO\text{-}B_2O_3\text{-}SiO_2$ glass. J Inorg Mater. 2017; 6(32): 643. (in China.)
[17]Lopes AAS, Monteiro RCC, Soares RS, Lima MMRA, Fernandes MHV. Crystallization kinetics of a barium–zinc borosilicate glass by a non-isothermal method. J. Alloys Compd. 2014;591(1): 268.
[18] Aroraa A, Goelb A, Shaaban ER, Singh K, Pandey OP, Ferreira JMF. Crystallization kinetics of $BaO\text{-}ZnO\text{-}Al_2O_3\text{-}B_2O_3\text{-}SiO_2$ glass. Physica B. 2008; 403(10–11): 1738.
[19] Imran MMA. Crystallization kinetics, glass transition kinetics, and thermal stability of $Se_{70-x}Ga_{30}In_x$ ($x$=5, 10, 15, and 20) semiconducting glasses. Physica B. 2011; 406(3): 482.
[20] Rafferty A, Hill R, Kelleher B, ODwyer T. An investigation of amorphous phase separation, leachability and surface area of an ionomer glass system and a sodium-boro-silicate glass system. J Mater Sci. 2003; 38(19): 3891.
[21] Hou ZX, Su CH. Composition, structure and optical properties of transparent glass ceramics. Shenyang: Northeastern University Press, 2008.
[22] Kullberg ATG, Lopes AAS, Veiga JPB, Lima MMRA, Monteiro RCC. Formation and crystallization of zinc borosilicate glasses: Influence of the $ZnO/B_2O_3$ ratio. J Non-Cryst Solids. 2016; 441: 79.
[23] Song XL, Hui XH. Fundamentals of Materials Science. Beijing: Chemical Industry Press, 2005.
[24] Huang J W, Li Z. X-ray Diffraction of Polycrystalline Materials-Experimental Principle, Method and Application. Beijing: Metallurgical Industry Press, 2012.
[25] Wang F, Liao QL, Zhu H Z, Dai YY, Wang H. Crystallization kinetics and glass transition kinetics of iron borophosphate glass and $CeO_2$-doped iron borophosphate compounds. J Alloys Compd. 2016; 686: 641.
[26] Kissinger HE. Variation of Peak Temperature With Heating Rate In Differential Thermal Analysis. J Res National Bureau Standards. 1956; 57(4): 217.

[27] Kissinger HE. Reaction kinetics in differential thermal analysis. Anal Chem. 1957; 29(11): 1702.
[28] Ozawa T. Estimation of activation energy by isoconversion methods. Thermochim Acta. 1992; 203(2):159.
[29] Augis JA, Bennett JE. Calculation of the Avrami parameters for heterogeneous solid state reactions using a modification of the Kissinger method. J Thermal Anal Calorim. 1978, 13(2): 283.
[30] Bai Y, Peng L, Zhu QS, Hao ZG. Non-isothermal crystallization kinetics of stoichiometric lithium disilicate-based glasses with $Al_2O_3$ additives. J Non-Cryst Solids. 2016; 445: 116.

**Graphic abstract:**

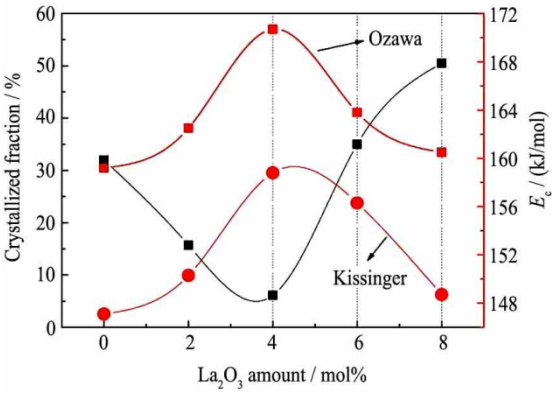


The dependence of the crystallization activation energy $E_c$ of $60ZnO\text{-}30B_2O_3\text{-}10SiO_2$ glass on the $La_2O_3$ doping amount is illustrated in the figure, the change trend of $E_c$ values estimated by Ozawa and Kissinger methods is the same, as the doping amount of $La_2O_3$ increases from 0 to 8 mol%, the maximum value of crystallization activation energy $E_c$ appears at 4 mol% of $La_2O_3$, indicating that the crystallization barrier needing to overcome is the largest for the glass doped with 4 mol% $La_2O_3$, as a result, the crystallization of glass is inhibited. This result can be used to control the depth of crystal layer on glass surface, crystallinity and thermal stability of $60ZnO\text{-}30B_2O_3\text{-}10SiO_2$ glass by doping with different contents of $La_2O_3$

## Declarations of interest

We declare that we do not have any commercial or associative interest that represents a conflict of interest in connection with the work submitted.